Refractive Index Sensor Based on Micro- Structured Optical Fibers with Using Finite Element Method

Amal I. Mahmood[1], Aseel I. Mahmood[2] [*], Sudad S. Ahmed[3]

[1]Department of Medical Instrumentation Engineering Techniques, Electrical Engineering Technical College, Middle Technical University, Baghdad, Iraq.
[2]Materials Research Directorate, Ministry of Science and Technology, Baghdad, Iraq.
[3]Physics Department, Science College, Baghdad University, Baghdad, Iraq.

Abstract

   In this paper a refractive index sensor based on micro-structured optical fiber has been proposed using Finite Element Method (FEM). The designed fiber has a hexagonal cladding structure with six air holes rings running around its solid core. The air holes of fiber has been infiltrated with different liquids such as water , ethanol, methanol, and toluene then sensor characteristics like ; effective refractive index , confinement loss, beam profile of the fundamental mode, and sensor resolution are investigated by employing the FEM. This designed sensor characterized by its low confinement loss and high resolution so a small change in the analyte refractive index could be detect which is could be useful to detect the change of the information of the biological molecule reaction and also in medical applications in fields like toxins, drug residues, vitamins, antibodies, proteins and parasites.

Keywords: MOF, FEM, RI- MOF sensor

استخدام طريقة العناصر المحددة لتصميم متحسس معامل الانكسار بالاعتماد على الالياف البصرية ذات الهيكلية الميكروية

امل إبراهيم محمود¹، اسيل إبراهيم محمود²، سؤدد سلمان احمد ³

¹ قسم هندسة تقنيات الأجهزة الطبية، الكلية التقنية الهندسية الكهربائية، الجامعة التقنية الوسطى، بغداد، العراق

²وزارة العلوم والتكنولوجيا، دائرة بحوث المواد، بغداد، العراق

³جامعة بغداد، كلية العلوم، قسم الفيزياء، بغداد، العراق

الخلاصة

   في البحث المقدم تم تصميم متحسس الياف بصرية لتحسس معاملات الانكسار للسوائل المختلفة بالاعتماد على طريقة العناصر المحددة. الليف المصمم يتميز بغلافه السداسي الشكل مع ستة حلقات هوائية تحيط حول القطر الصلب، تم ملئ هذه الفجوات بسوائل ذات معاملات انكسار مختلفة مثل الماء، الايثانول، الميثانول والتولين. تم دراسة الخصائص البصرية لهذا المتحسس وهي معامل الانكسار المؤثر خسائر الحصر للأنماط الأساسية وكذلك دقة المتحسس. المتحسس المصمم يتميز بخسائر حصر قليلة ودقة عالية أي ان تغير بسيط في معامل انكسار المحلل يمكن تحسسه بهذا التصميم وهذا مهم في تحسس التغير في تفاعلات الجزيئات البيولوجية وكذلك في التطبيقات الطبية الأخرى كالكشف عن السموم ومخلفات الادوية، الفيتامينات ، الاجسام المضادة، البروتين والطفيليات.

_____

*Email: aseelibrahim208@gmail.com

الكلمات المفتاحية: الليف البصري ذو الهيكلية المايكروية، طريقة العناصر المحددة، متحسس معامل الانكسار

بالألياف البصرية ذات الهيكلية المايكروية.

Introduction

Optical fiber sensors have wide applications in science, the environmental monitoring, and communication technology this is due to their compact in size, high sensitivity, electrical passiveness, immune to electromagnetic interference, wide bandwidth as well be made convenient for tip-based sensing. Most of these optical sensors measure the variations of optical properties because of a change in the refractive index (RI) of a gas or a liquid [1]. Measuring the RI of fluids is very important; so as to depict the optical properties of fluids which is lead to evolution of RI sensors for applying in many fields such as the salinity of water measurement [2], and biotechnology processes [3] also provide important acquaintance on drug/DNA interaction and growth of the cell [4]. Anew type of optical fiber had been developed in the beginnings of nineteenths, called Micro-Structured Optical Fibers (MOF) or Photonic Crystal Fibers (PCFs), in which air holes were developed along the fiber structure [5]. Micro- Structured could be classified according to the guiding mechanism to; index- guiding and band-gab MOF's. The first type, the core is solid and the cladding is represented by two- dimensional lattices of air holes running along the entire length of the fiber. The RI of the index –guiding MOF is higher than the cladding, so the light will be guided inside the fiber core by means of total internal reflection [6], while in band-gap type the light will be guided by a two- dimensional photonic band-gab because the core in these fibers is air or (hollow core) which its refractive index less than the refractive index of cladding. Due to the band- gab phenomena specific frequencies of light that propagate along the fiber are not allowed to escape from the core but will be reflected and constructively interference inside the core and destructively interference in the cladding [7]it, Figure -1 shows some types of MOFs.
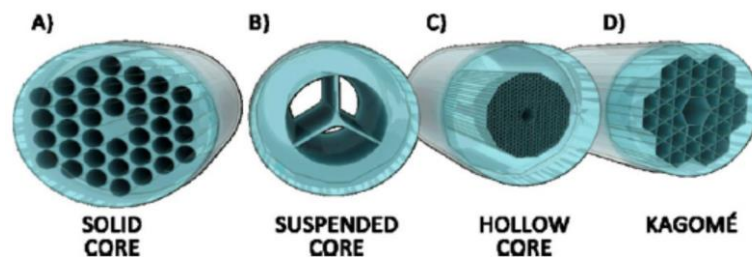
Figure 1-Some typical structures of MOFs (A) Solid Core-MOF, (B) Suspended core MOF; (C) Hollow Core-MOF, and (D) Kagom´e HC-MOF [8].

The unique properties of MOFs lead to developed different and new schemes of optical RI-sensors; a microfluidic RI sensor based solid-core PCF presented by Wu et al. , the RI sensitivity was circa 38,000 nm/RIU [9]. Park et al. implemented a MOF-based reflection kind refractometer insensitive to temperature for RI measurement the sensitivity was 850 nm/RIU [10], and Li et al. [11] attained an optimum sensitivity of 1629 nm/RIU by developing instead a tapered-PCF in transmission. In addition, the unique geometrical structure of MOF allows tuning of propagation properties of the fiber via alteration the air hole position, size and shape [8]. The Sensitivity and the confinement loss considered as the main guiding properties of MOF sensors. Several simulation works that used FEM have been published to gain sensitivity at a maximum and confinement loss at a minimum suitable grade in the environmental and biological sensing applications. Olyaee et al. designed index-guiding-MOF for gas sensing and they achieved lower dispersion, confinement loss and nonlinear effect simultaneously [12]. Cordeiro et. al submitted a new concept for evanescent sensing application in which both the core and the cladding are micro- structured [13]. Octagonal- MOF with smaller loss and the higher prorated sensitivity coefficient for three analytes like Water, Ethanol and Benzene had been submitted by Ademgil [14].

Kawser et al. designed an O-PCF structure with high relative sensitivity and low confinement loss and investigated the effects of different parameter variations on propagation properties over a wide wavelength range [15], also high sensitivity, high nonlinearity, high birefringence and low confinement loss MOF submitted by Arif et al. 2017 which both core and cladding are micro-structured the core of the MOF structure is designed with two rows of supplementary elliptical air hole.

Materials and Methods

In this work, an index guided MOF with hexagonal shaped air holes rings in the cladding area had been designed. The number of air hole rings were six, normalized air hole size (d/Λ) was 0.4, hole to hole spacing (Λ) circa 7.5μm, air hole diameter (d) 4 μm, and core diameter (ρ) 10 μm, Figure-2 shows the designed fiber.
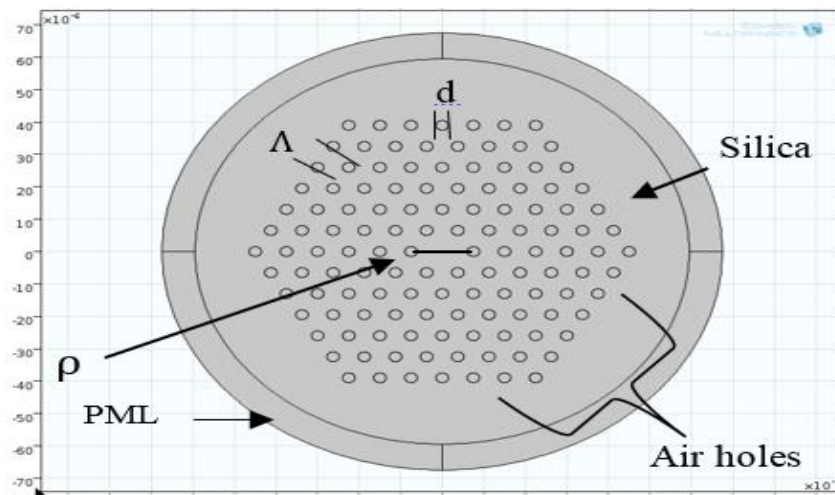
Figure 2-Schematic illustration of the proposed MOF.

Finite Element Method (FEM) with Perfectly Matched Layer (PML) boundary condition is depended for the analysis of the structure with a FEM based simulation software COMSOL Multiphysics 4.4, FEM provides the effective investigation of MOF dispersion, amplification and nonlinear properties. Moreover, the complex formula of FEM so beneficial, for instance, to evaluate the MOF leakage or confinement losses, because of the finite number of air-hole rings in the cladding lattice, the following equation with a magnetic field formulation can be derived from the Maxwell equations [16]:

$$\nabla \times \left(\mu_r^{-1}\nabla \times \vec{E}\right) - k_0^2 \varepsilon_r \vec{E} = 0 \tag{1}$$

This is an eigen value equation, the eigen values are (β/k_0) the effective indices(n_{eff}), and the eigenvectors are the electric field components (E_x, E_y, E_z). In (1), $(\vec{E})$ represent the electric field, (k_0) represent the wave number in vacuum, and (ε_r) and (μ_r) are the dielectric permittivity and magnetic permeability tensors, respectively [16].

The modal analyzes performed on the x-y plane cross sectional MOF structure as the wave is propagating in the z direction. The MOF cross-sectional in the transverse X – Y plane is divided into triangular elements with different shapes, sizes, and refractive indices. Any type of geometry, inclusive the MOF air-holes, as well as the characteristics of the medium, can be precisely described. In particular, the FEM is adequate for analyzing fibers with nonperiodic air-hole arrangements. As well as, it provides a full-vector analysis which is requisite to model MOFs with large air-holes and high index changes, and to predict precisely their properties.

The attenuation resulted from the waveguide geometry is called the confinement losses or leakage losses L_c ; confinement losses originates from the finite width of the cladding structure. This is an extra type of losses that happened in single material fibers especially in MOFs because they are commonly made of pure silica, L_c in dB/m is given by [17]

$$L_c = -20\log_{10} e^{-k_0 Im[n_{eff}]} = 8.686 k_0 Im[n_{eff}] \tag{2}$$

where (k_0) is the propagation constant in free space, and Im[n_{eff}] is the imaginary part of the complex effective refractive index (n_{eff}).

In this work, the air holes of the designed MOF was infiltrated with water, ethanol, methanol, and toluene then confinement loss, the effective refractive index, and the sensor resolution have been studied for each case.

Results and discussion

To analyze the sensor characteristics, a large analyte RI range from 1to 1.48 is investigated at 1-1.7 μm wavelength. The MOF cladding which is a two-dimensional photonic crystal with 6- rings of the hexagonal lattice air holes in the silica matrix have been infiltrated with different liquids (water, ethanol, methanol, and toluene) which have different refractive indices. Then the numerical analyses on some propagation characteristics of the proposed MOF structures in fundamental mode have been studied.

Figure-3, shows the electric field profile for wavelengths ((a) 1, (b) 1.55, (c) 1.3, and (d) 1.7 μm) in absence of the analyte, while Figure-4 shows the real part of the effective index Re (n_{eff}) variations with the operating wavelength, and Figure-5 shows the confinement loss behavior with wavelength which is remains at around 0 dB/m due to high confinement of mode.

Figures-(6,9,12, 15) show the electric field profile for wavelengths ((a)1, (b)1.55,(c)1.3, and (d) 1.7 μm)) of samples infiltrated with analyte water, ethanol, methanol, and toluene respectively. It can be noted that the electric field is fundamentally confined in the MOF core region.

Figures-(7,10,13, 16) illustrates the variation of the real part of the effective index Re (n_{eff}) with the operating wavelength, for samples infiltrated with water, ethanol, methanol, and toluene respectively, At longer wavelengths, Re (n_{eff}) is low, while it is inversely proportional wavelength.

Figures- (8, 11, 14, 17) shows the confinement loss against wavelength for the proposed MOF structure infiltrated with water, ethanol, methanol, and toluene respectively.

The refractive index resolution (R) of the corresponding sensor can be obtained as: [18]

$$R = \Delta n_a \Delta \lambda_{min} / \Delta \lambda_{peak} \tag{3}$$

Where $\Delta \lambda_{min}$ peak-wavelength resolution is assumed to be $\Delta \lambda_{min} = 0.1$ nm, Δn_a the variation of the analyte refractive index, and $\Delta \lambda_{peak}$ the variation of the peak wavelength.

according to above equation, the resolution for the submitted sensor is about 2.33x10^{-7} RIU, 6 x10^{-7},1.27 x10^{-7} RIU, 1.48 x10^{-7} RIU and 6.9 x10^{-7} RIU for samples infiltrated with air, toluene, methane, ethanol, and water respectively.
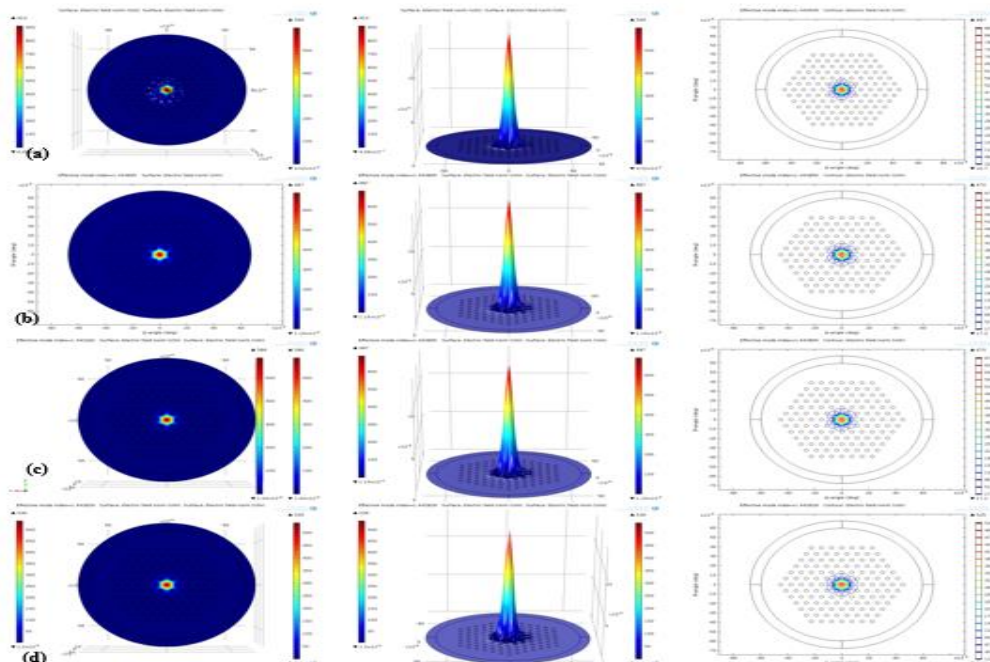
Figure 3- Electric field profile of the MOF without analyte with different wavelength,(a) 1μm, (b) 1.3 μm, (c) 1.55 μm and (d) 1.7 μm.
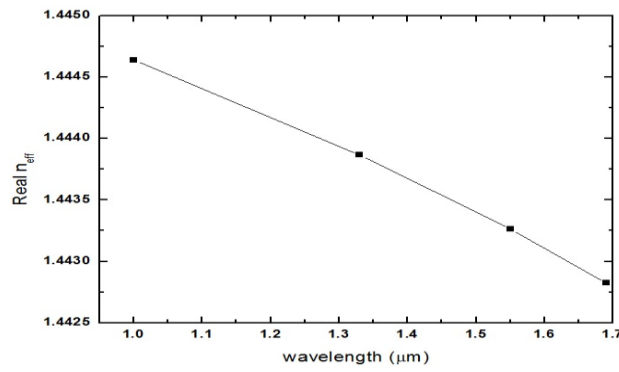
Figure 4-The real part of n_{eff} of the fundamental mode as a function of operated bandwidth.
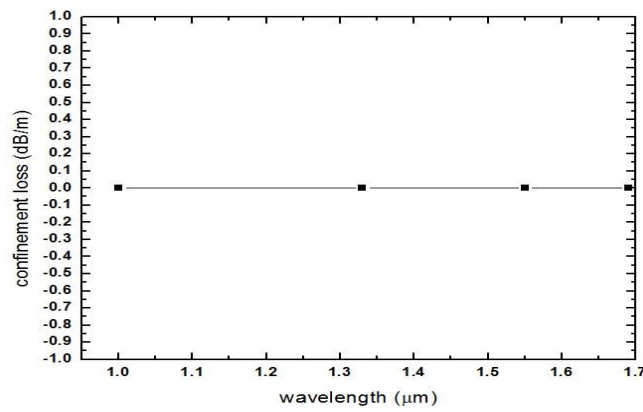
Figure 5- The simulated L_c of the fundamental mode as a function of operated band width.
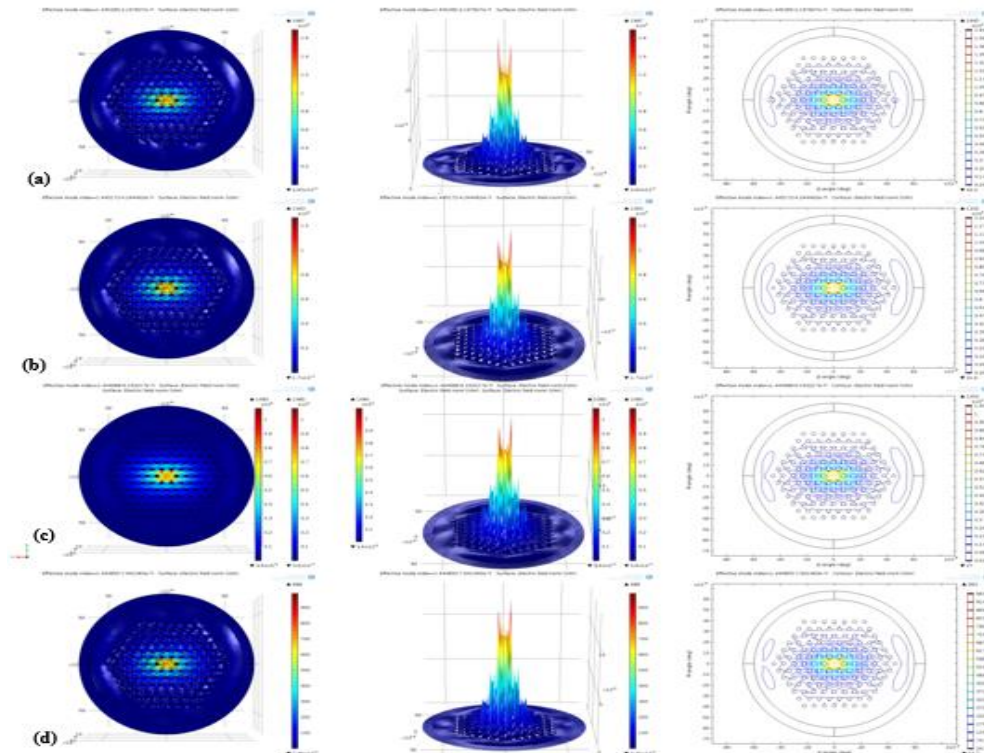
Figure 6-Electric field profile of the MOF infiltrated with water of different wavelength,(a) 1µm, (b) 1.3 µm, (c) 1.55 µm and (d) 1.7 µm.
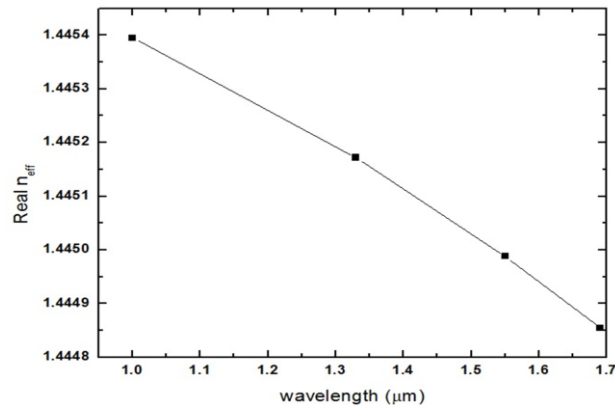
Figure 7-The real part of n_{eff} of the fundamental mode as a function of operated bandwidth.
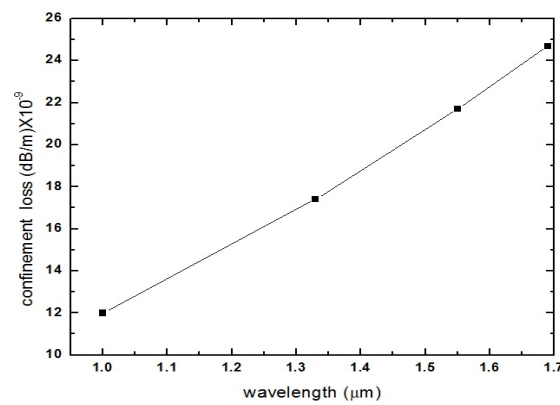
Figure 8- The simulated L_c of the fundamental mode as a function of operated band width.
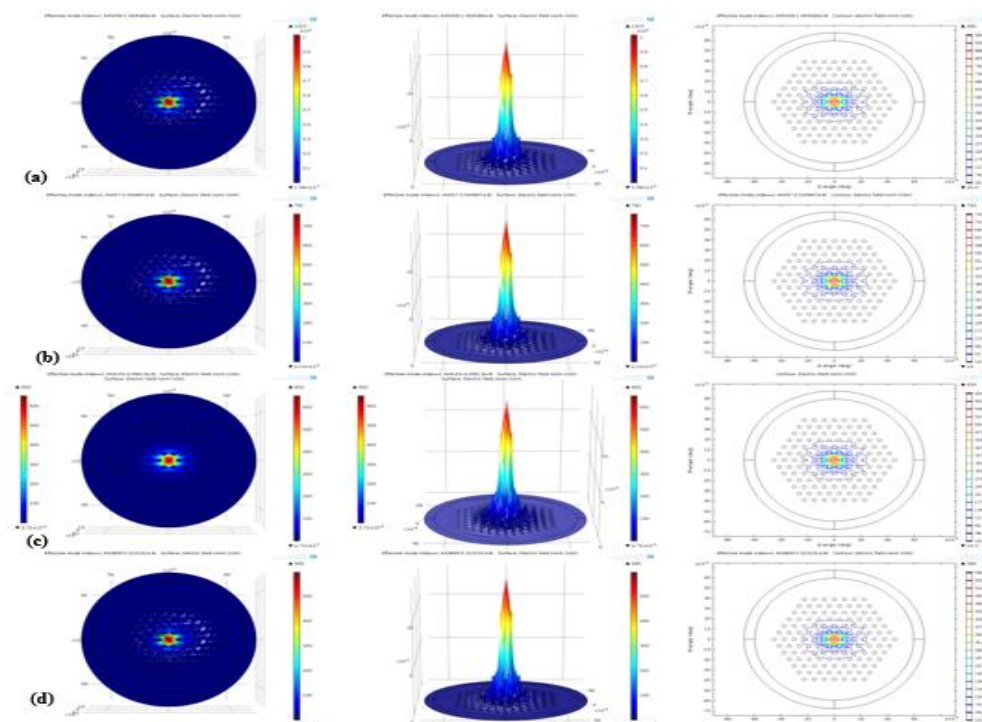
Figure 9-Electric field profile of the MOF infiltrated with ethanol of different wavelength,(a) 1µm, (b) 1.3 µm, (c) 1.55 µm
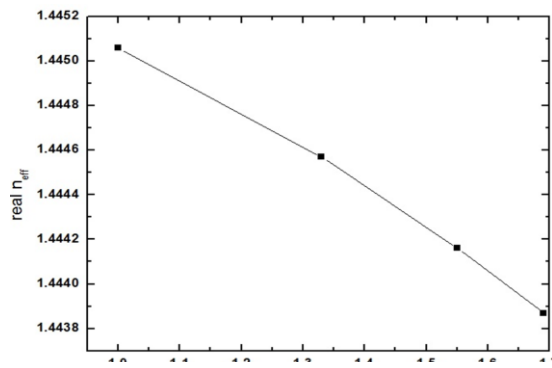
Figure 10-The real part of n_{eff} of the fundamental mode as a function of operated bandwidth.
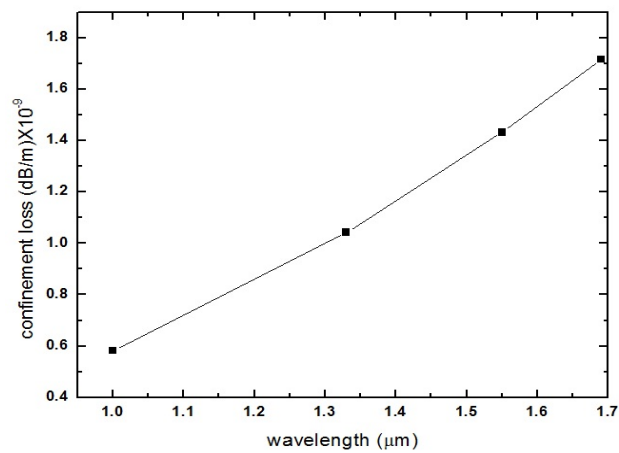
Figure 11-The simulated L_c of the fundamental mode as a function of operated bandwidth.
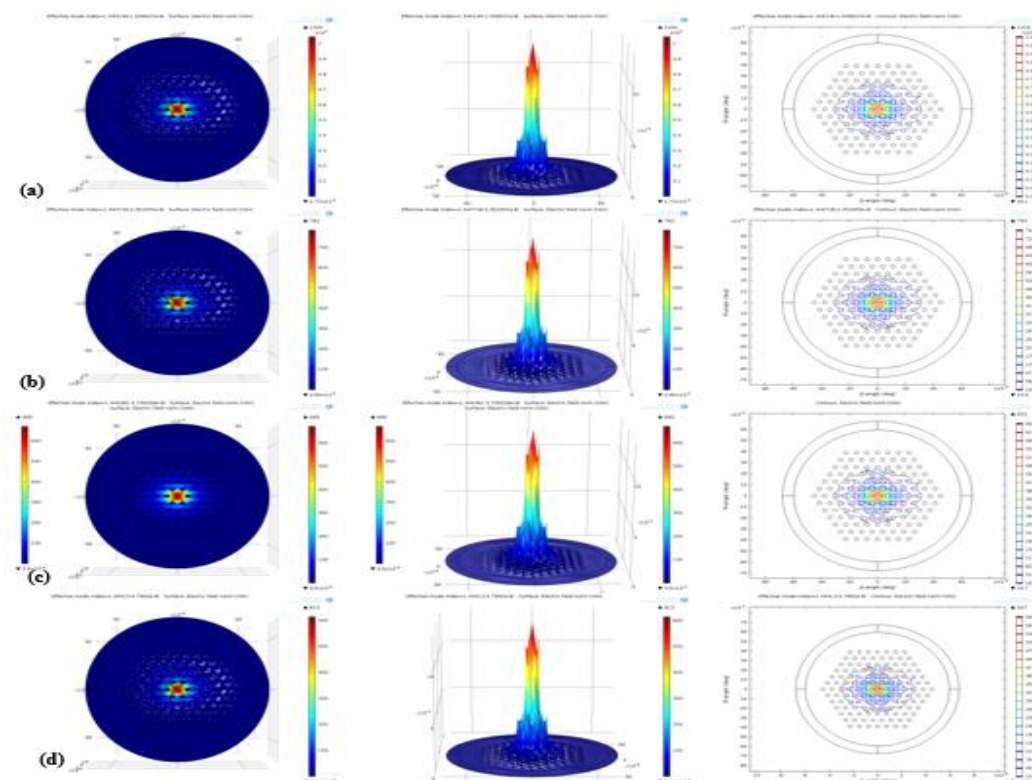
Figure 12- Electric field profile of the MOF infiltrated with methanol of different wavelength,(a) 1μm, (b) 1.3 μm, (c) 1.55 μm and (d) 1.7 μm.
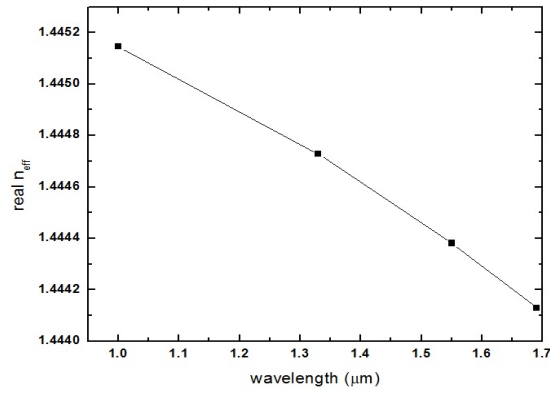
Figure 13-The real part of n_{eff} of the fundamental mode as a function of operated bandwidth.
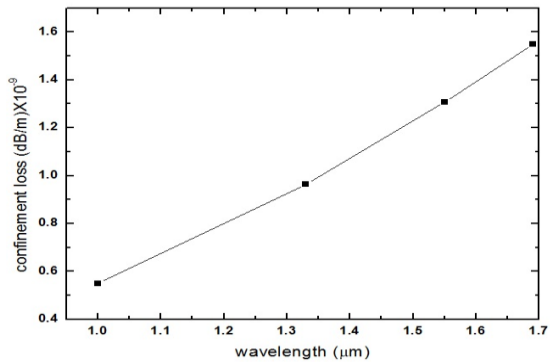
Figure 14-The simulated L_c of the fundamental mode as a function of operated bandwidth
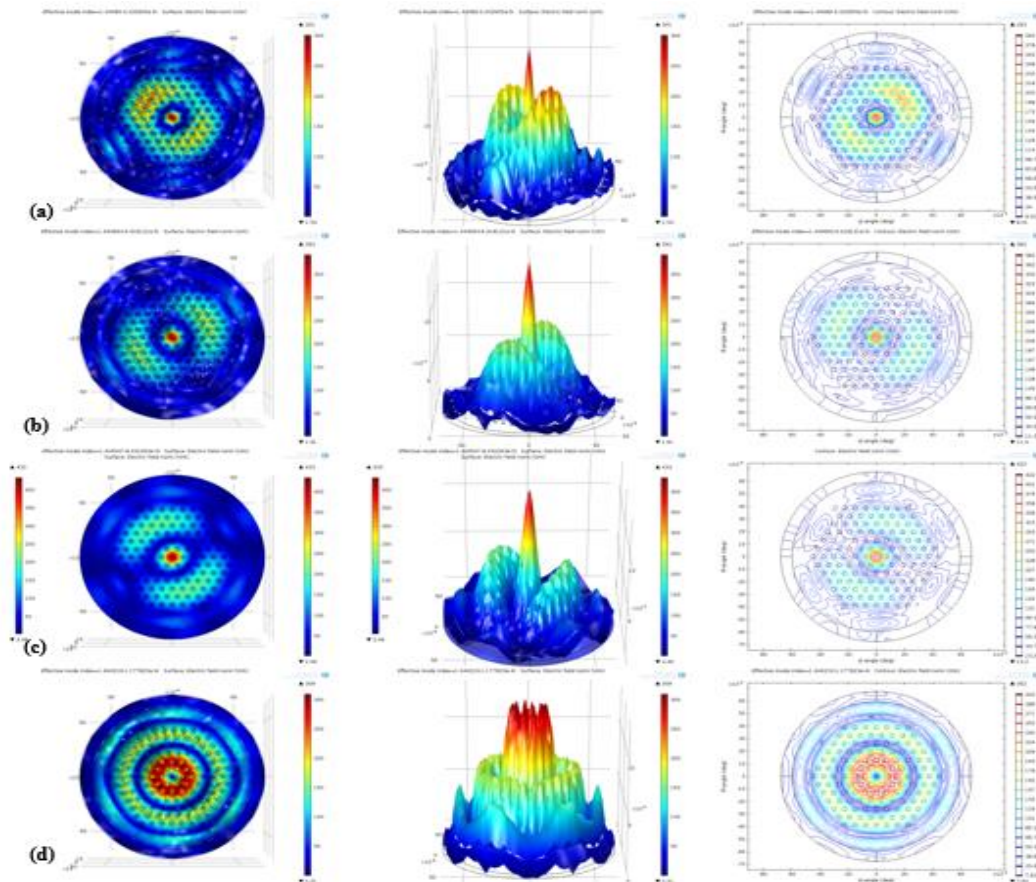
Figure 15-Electric field profile of the MOF infiltrated with toluene of different wavelength,(a) 1µm, (b) 1.3 µm, (c) 1.55 µm and (d) 1.7 µm.
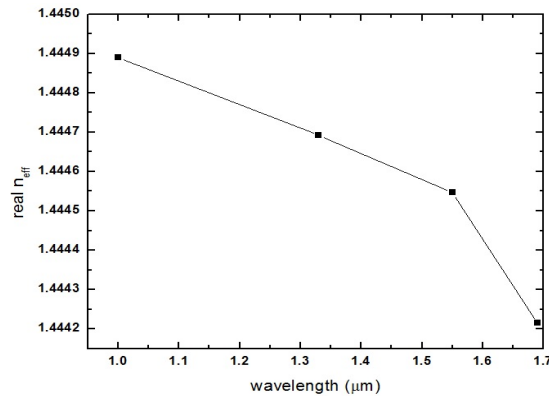
Figure 16-he real part of n_{eff} of the fundamental mode as a function of operated bandwidth.
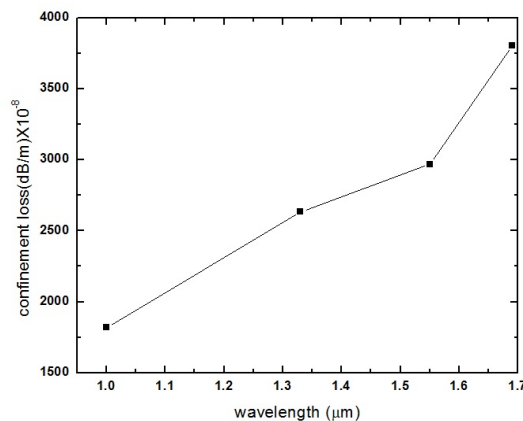
Figure 17-The simulated L_c of the fundamental mode as a function of operated band width.

The characteristics of the effective refractive index of the proposed structures have been studied. The numerical investigation for all samples shows the effective index profiles of the proposed micro-structured fiber at different wavelengths. An increase in the operating wavelength results in a linear decrease in effective indices. The confinement losses calculated according to eq. 2, from the results for empty samples high confinement had been obtained; no leakage loss obtained. For the infiltrated samples the confinement loss is increase by the increasing of wavelength; this could be explain as effective refractive index of the fundamental mode began to reach to refractive index of pure silica (at shorter wavelength) propagation become parallel to the fiber axis so the interaction with holly structure will be minimized.

Conclusion

A refractive index sensor based on MOF with hexagonal lattice was suggested. Numerical analysis of the designed fiber is carried out by FEM. For all samples the effective refractive index was decreased with increasing of the wavelength range, also the fundamental modes are highly confined in core region for the samples infiltrated with liquids which their RI is less than the RI of silica (it's about 10^{-9} dB/m); the light is propagate according total internal reflection , while for toluene sample with RI is about 1.48 which is higher than the RI of silica the modes will be widely leakage out of the MOF core (confinement loss about 10^{-6} dB/m) the light will be guided according photonic band gap effect, also this sensor has a high resolution (about 10^{-7} RIU). This MOF RI-sensor could be used in various medical and environmental sensing applications using different fluids analytes due to its high resolution and low confinement loss.

References
1. Mohebbi, M**. 2015.** Refractive index sensing of gases based on a one-dimensional photonic crystal nanocavity. *Journal of Sensors and Sensor Systems*, **4**: 209–215. Doi: 10.5194/jsss-4-209-2015.
2. Pereira, D., Frazão, O. and Santos, J. **2004**. Fiber Bragg grating sensing system for simultaneous measurement of salinity and temperature. *Optical. Engineering*, **43**: 299–304.
3. Jiménez-Márquez, F., Vázquez, J., Úbeda, J. and Sánchez-Rojas, J. **2013**. Low- cost and portable refractive opteoelectronic device for measuring wine fermentation kinetics. *Sensors and Actuators B Chemical*, **178**: 316–323.
4. Silva, S., Roriz, P. and Frazão, O. **2014**. Refractive index measurement of liquids based on microstructured optical fibers. *Photonics*, **1**: 516-529. Doi:10.3390/ photonics1040516.
5. Birks, T., Knight, J., and Russell, P. 1997. Endlessly single-mode photonic crystal fiber. *Optics Letters*. **22**: 961–963.
6. Pristinski, D. and Du, H. **2006**. Solid-core photonic crystal fiber as a Raman spectroscopy platform with a silica core as an internal reference. *Optics letters*, **31**: 3246-3248. Doi:10.1002 /lpor.201500045
7. Benabid, F., Knight, J., Antonopoulous, G., and Russell, P.**2002**. Stimulated Raman scattering in hydrogen-filled hollow-core photonic crystal fiber. *Science*, **298**(5592): 399-402. Doi:10.1126/science.1076408
8. Calcerrada, M., Garc´ıa-Ruiz, C. and Gonz´alez-Herr´aez, M. **2015**. Chemical and biochemical sensing applications of microstructured optical fiber – based systems. *Laser and Photonics Reviews*, **9**: 604–627.
9. Wu, D., Kuhlmey, B. and Eggleton, B.**2009**. Ultrasensitive photonic crystal fiber refractive index sensor. *Optics Letters,* **34**: 322–324. Doi:10.1364/OL.34.000322.
10. Park, K., Choi, H., Park, S., and Lee, B. **2010**. Temperature robust refractive index sensor based on a photonic crystal fiber interferometer . *IEEE Sensors Journal*, **10**: 1147–1148.
11. Li, C., Qiu, S.-J. , Chen, Y., Xu, F. and Lu, Y.-Q. **2012**. Ultra-sensitive refractive index sensor with slightly tapered photonic crystal fiber. *IEEE Photonics Technology Lett*ers, **24**:1771–1774.
12. Olyaee, S., Seifouri, M., Nikoosohbat, A. and Abadi, M. **2015**. Low nonlinear effects index-guiding nanostructured photonic crystal fiber. *World Academy of Science, Engineering and Technology International Journal of Electronics and Communication Engineering.* **9**: 253–257.
13. Cordeiro, C., Franco, M. , Chesini, G., Barretto, E., Lwin, R., Brito Cruz, C.H. and Large, M. **2006.** Microstructured-core optical fiber for evanescent sensing applications. *Optics Express*, **14** **:** 13056–13066 **.** Doi.10.1364/OE.14.013056
14. Ademgil, H. **2014**. Highly sensitive octagonal photonic crystal fiber based sensor. *Optik International Journal for Light and Electron Optics*. **125**: 6274–6278.
15. Ahmed, K. and Morshed, M. **2016**. Design and numerical analysis of microstructured-core octagonal photonic crystal fiber for sensing applications. *Sensing and Bio-Sensing Research*, **7**: 1–6. Doi:10.1016/j.sbsr.2015.10.005
16. Arif, Md. F. and Biddut, Md. J. **2017**. A new structure of photonic crystal fiber with high sensitivity, high nonlinearity, high birefringence and low confinement loss for liquid analyte sensing applications. *Sensing and Bio-Sensing Research*, **12**: 8–14.
17. Finazzi, V., Monro, T., and Richardson, D.**2003**. The role of confinement loss in highly nonlinear silica holey fibers. *IEEE Photonics Technology Letters*, **15**: 1246 – 1248.
18. Wang, H., Yan, X., Li, Sh., An, G. and Zhang, X. High sensitivity refractive index sensor based on dual-core photonic crystal fiber with hexagonal lattice. **2016**. *Sensors*, **16**: 1655(1-10). Doi: 10.3390/s16101655.